ELSEVIER

## Contents lists available at ScienceDirect

## **Hybrid Advances**

journal homepage: www.journals.elsevier.com/hybrid-advances



## Research Article

# Heavy metal removal from wastewater using functionalized nano-structures and graphene oxide

Amar Yasser Jassim<sup>a</sup>, Balqees Suhaem Al-Ali<sup>b</sup>, Wesam R. Kadhum<sup>c</sup>, Ehsan kianfar<sup>d,\*</sup>

- <sup>a</sup> Department of Marine Vertebrate, Marine Science Center, University of Basrah, Basrah, 61001, Iraq
- <sup>b</sup> Depth. of Chemistry and Marine Environment Pollution, Marine Science Center, University of Basrah, Iraq
- <sup>c</sup> Department of Pharmaceutics, College of Pharmacy, University of Kut, 52001, Wasit, Iraq
- <sup>d</sup> Young Researchers and Elite Club, Gachsaran Branch, Islamic Azad University, Gachsaran, Iran

#### ARTICLE INFO

#### Keywords: Graphene oxide Heavy metals Wastewater treatment Environmental pollution Absorption

#### ABSTRACT

Toxic heavy metals present in aqueous media threaten the survival of human beings and ecosystem, but mechanisms underlying their absorption by nanoparticles are limitedly studied. The  $Pb^{2+}$ ,  $Cu^{2+}$  and  $Cd^{2+}$  are taken as characteristic of heavy metals, while pristine and amine-functionalized graphene oxide (GO) nanosheets as absorbents. The combination of bench- and computer-based studies unraveled the effects of chemistry and thermodynamics of model heavy metals absorption by GO. Synthesis of 6-aminouracil functionalized GO (GO-A) and ethylenediamine functionalized GO (GO-E) reveled the higher potential of GO-E compared to GO and GO-A towards absorption of  $Pb^{2+}$ ,  $Cu^{2+}$  and  $Cd^{2+}$ , following the order GO-E > GO-A > GO. The topmost absorption capacity varied with pH of the solution, where the highest absorption capacity of GO-E towards  $Cd^{2+}$  was evident, i.e. four to five times higher than those of  $Pb^{2+}$  and  $Cu^{2+}$ . Furthermore, the desorption behavior of the heavy metal ions from the GO surface was significant, indicating that GO could be reused after treated with hydrochloric acid solution. Gibbs free energy computations unraveled that  $Cd^{2+}$  was spontaneously adsorbed to nanosheets compared to  $Pb^{2+}$  and  $Cu^{2+}$ . The role of surface chemistry was unraveled with GO-E compared to GO and GO-A in both gas and solvent phases.

## 1. Introduction

From the time industrial revolution was announced in Britain and gained momentum, the human health issues being triggered by industrialization have always been beyond remedy [1-4]. Alongside population growth and urbanization, facilitated modernization of the textile, iron, mining, chemicals, and agricultural industries have altogether flourished the enterprise development leading to drastic economic growth [5–9]. By contrast, industrial effluents have made serious threats against the environment and human beings, which criticized the sustainability and circularity of materials and manufacturing processes [10-13]. Heavy metal pollution holds a top position among industrial toxic materials, quickly and harmfully spread through the ecosystem, subsequently endanger the survival of plants, animals and humans [14–17]. For example, chemical and mining industries are main reasons for cadmium (Cd<sup>2+</sup>) spread through water resources [18–20]. However, inorganic Arsenic (As) originating from natural resources enters groundwater through dissolving into the soil, subsequently accumulates into crops such as rice and corn largely consumed by the humans [21–24]. An elaborated study based on detailed analysis of global data collection over the last 50 years from rivers and lakes has alerted the public to the dangers of heavy metal concentrations and sources [25–30]. Overall, the aforementioned decadal survey from 1970s to 2010s (1972–2017) was indicative of global increase in both the concentration and multiplicity of heavy metals in aquatic environments based on standards of World Health Organization (WHO). Moreover, the survey underlined mining, manufacturing, fertilizer and pesticide as the major heavy metal pollution sources depending on the region. Fig. 1 summarizes the main heavy metals sources worldwide and their corresponding sub-categorized industries [5].

When it comes to wastewater decontamination, the spread, circularity, and pollution cycle of heavy metals should simultaneously be taken into consideration [31–34]. The noxious spread of hazardous compounds through the environment originates from anthropogenic activities, which are reflected in COx/NOx/SOx emissions, industrial wastewater and soil contamination affecting heavy metals circulation

E-mail addresses: ehsan\_kianfar2010@yahoo.com, ehsankianfar775@gmail.com (E. kianfar).

<sup>\*</sup> Corresponding author.

(Fig. 2A). Heavy metals pollution fueled by poor effluent management has devastating consequences for plants, animals, and humans beings [35-39]. The toxicity consequences of heavy metals should be critically viewed alongside their non-biodegradability in the ecosystem. Moreover, heavy metal ions entering human food chain are toxic in all forms, either free or complexed, even at low concentrations. Through formation of complex compounds within the human cells, heavy metals substantially disrupt their metabolic and endocrine functions [40-42]. A multitude of diseases ranging from allergic dermatitis and skin reactions to developmental retardation, immunological and neurological disorders, tissue damage and cancer are the consequences of heavy metal circulation in the ecosystem (Fig. 2B) [8,9]. For instance, approximately one third of Cd<sup>2+</sup> entering human body are stored in the kidneys, leading to coagulation of urea proteins and blockage of kidney ducts and tubes, and also acceleration of kidney stones formation [43,44]. The  $Cd^{2+}$ accumulation in the liver disables some enzymes, which becomes more critical with age [45,46]. Basic information required for health risk assessment of reuse of heavy metals contaminated industrial wastewaters for irrigation has elaborated in a review paper [12]. However, the mechanism of devastating effects of combination of heavy metals in living organisms remains a hot debate.

In the light of above discussions, the detection, recycling, and removal of heavy metals from industrial wastewater appears important from both environmental and economic perspectives. Recently, various technologies such as ion exchange, chemical deposition, evaporation, reverse osmosis and electrochemistry have been served to separate heavy metal ions from industrial wastewaters [13,14]. However, there are limitations in using these methods such as low selectivity, low capacity to collect metal ions, and producing other toxic compounds [15]. Unlike the aforementioned strategies, absorption methods are best known for their efficiency from an economic point of view, which can be engineered depending on the application and through adjustment of the affinity between the adsorbent and the target pollutants. Carbonaceous absorbents have been widely used for heavy metal removal because of their wide range of variety as well as regional and global availability. Due to the cationic nature of heavy metal ions, carbon-based absorbents

with acidic pH are prioritized. Nevertheless, physical absorption, electrostatic interaction, ion exchange, surface complexation, and participation are known as possible absorption mechanisms for removal of individual or coexisting heavy metals in wastewater [17]. In parallel with worldwide interest in the use of nano-absorbents in heavy metals removal from wastewater over the last two decades [18], both pristine and functionalized carbon-based nano-absorbents were repeatedly examined [19]. Graphene based nano-absorbents has been recently considered with many scientists worldwide for their ability to absorb heavy metal ions from wastewater originating from their high cross-sectional area, and ability to be functionalized with diverse functional groups [20].

Zeng et al. [51] Oxytetracycline (OTC) and sulfamethoxazole (SMX) coexisting in aquatic settings may experience competing absorption to affect the removal efficacy of NAC, a developing carbonaceous nanomaterial for water treatment. Using density function theory (DFT) calculations and experimental analysis, this work examined the competitive absorption of OTC and SMX onto NAC under various interaction sequence, pH, electrolyte, and water matrix conditions. According to absorption kinetics, the absorption of one antibiotic was reduced by an increase in its concentration. Due to competitive absorption, binary systems reached equilibrium more quickly than single systems, and the pseudo-second-order model matched both systems the best. NAC seemed to have a greater affinity for OTC (395.26 mg/g) than SMX (232.02 mg/g), according to absorption isotherms, and the Langmuir model fit both single and binary systems. Sequential absorption of [NAC + OTC] + SMX was preferred to binary absorption, which is consistent with the optimal SMX-[NAC-OTC±] structure with a binding energy of -57.25 kcal/mol derived from DFT calculations. The pH range of 3.2-5.6 was ideal for competitive absorption since this is where NAC and cationic antibiotics were electrostatically attracted to one another. Competitive absorption was affected by salting-out, charge screening, and complexation effects from Na<sup>+</sup> and Ca<sup>2+</sup>. In both single and binary systems, NAC was able to remove OTC and SMX from wastewater effluent among four water matrices in the most efficient manner. Absorption was facilitated by hydrogen bonding,  $\pi - \pi$  electron

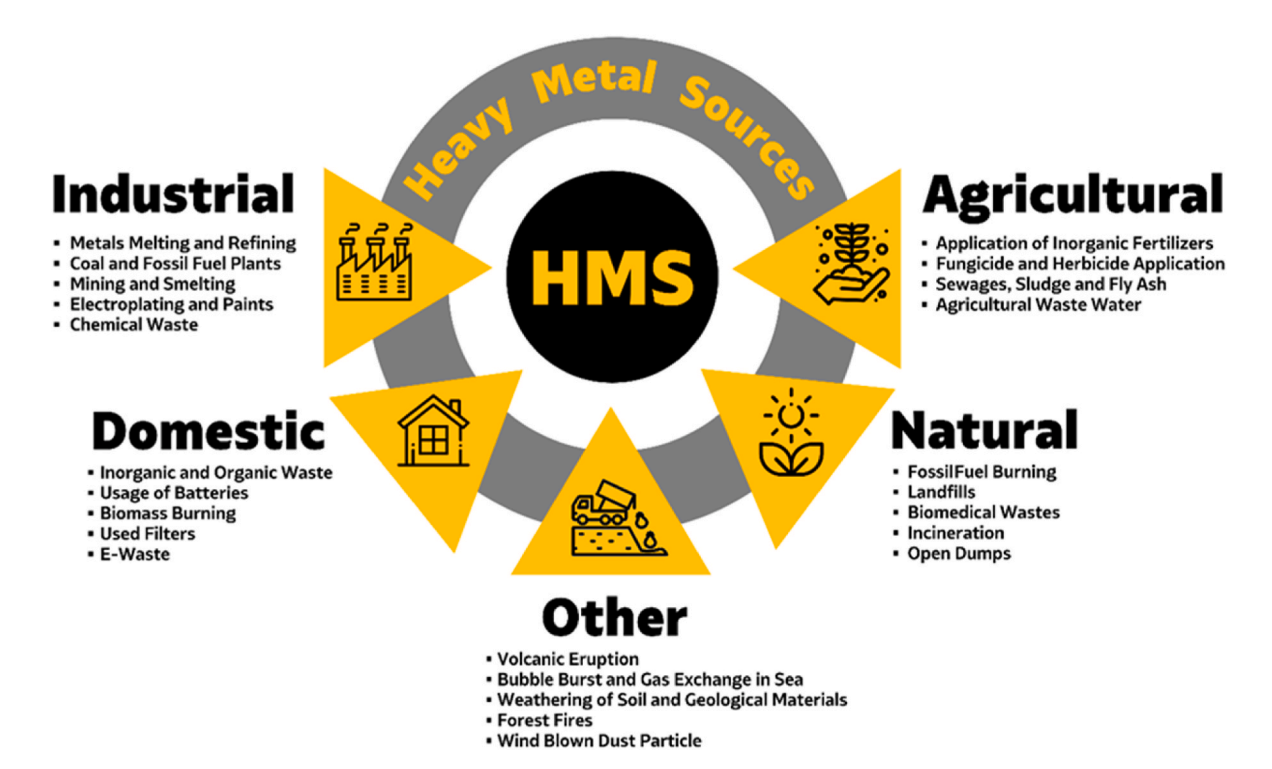
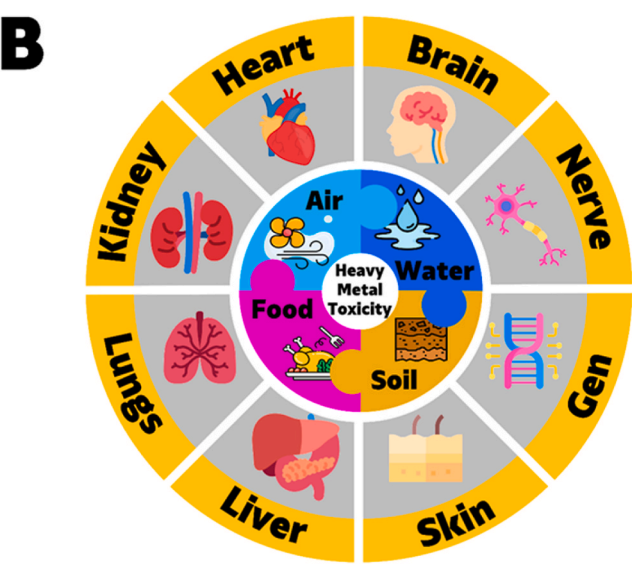


Fig. 1. A brief overview of main sources of heavy metals from industrial, agricultural, domestic, natural, and other or miscellaneous sectors alongside some anthropogenic sub-categories of pollutant industries.

Hybrid Advances 11 (2025) 100552





**Fig. 2.** (A) Global view of circulation of heavy metals in the ecosystem; and (B) heavy metal spread through soil, water, air, and food chain correlated with sediments in human tissues and organs from food chain.

donor–acceptor interactions, hydrophobic interactions, and electrostatic interactions. The functional groups of NAC underwent a sequential transition in single and binary systems, respectively, after - OH  $\rightarrow$  C - H  $\rightarrow$  C - O  $\rightarrow$  C=C and C=C  $\rightarrow$  C - O  $\rightarrow$  C - H  $\rightarrow$  OH. The results demonstrate NAC's potential for remediating antibiotic combinations in complicated aquatic settings and offer important insights into the competitive absorption processes of antibiotics on NAC.

Gallego-Villada, Luis A. et al. [52] Using a dendritic ZSM-5 zeolite (d-ZSM-5) as a highly selective catalyst for the synthesis of dihydrocarvone (DHC) in the form of diastereoisomers (cis + trans), this work investigates the isomerization of limonene-1,2-epoxide (LE) from kinetic and mechanistic perspectives. Green solvent ethyl acetate was employed at moderate reaction temperatures (between 50 and 70  $^{\circ}$ C). DHC, which may also be derived from caraway oil, is a common ingredient in tastes and fragrances as well as an intermediary in the synthesis of epoxylactone. Using a reaction network including eight parallel reactions and the associated rate equations, which were obtained from the assumption of the rate-limiting surface reactions, kinetic modeling of LE isomerization was carried out. Three of those processes

may be disregarded in order to more properly characterize the kinetic model, according to the statistical results of several kinetic parameters of the first data fitting, which showed substantial standard errors. The statistical dependability of the improved kinetic model was confirmed by this refinement, which produced standard errors in the kinetic parameters that were less than around 11 %. The calculated activation energies for the production of *trans*-DHC and *cis*-DHC were 162 and 41.1 kJ/mol, respectively. The optimum route for the conversion of both cis and *trans*-LE to DHC and carveol was determined using Density Functional Theory (DFT) calculations. Near-instantaneous dihydrocarvone production occurs under the examined conditions after the rate-determining step of carbocation formation ( $\Delta$ Eact = 234 kJ/mol).

Xi Wang et al. [53] The direct and efficient removal of multiple heavy metal ions from acidic wastewater are a challenge. In this study, an efficient adsorbent of polyvinyl alcohol with abundant phosphate functional group (P-PVA) was designed and prepared for the simultaneous removal of multiple heavy metal ions (i.e., Cd2+, Cu2+, and Pb2+) from acidic wastewater. The characterization results indicated that abundant phosphate functional groups can be grafted with polyvinyl alcohol. Under acidic conditions (pH = 3), the absorption results of P-PVA adsorbent show rapid removal of Cd<sup>2+</sup>, Cu<sup>2+</sup>, and Pb<sup>2+</sup>. The maximum absorption capacities of 210.21 mg/g, 140.76 mg/g, and 235 mg/g were obtained for Cd2+, Cu2+, and Pb2+ ions, respectively. The adsorbent also shows high absorption capacity in the presence of humic acid or coexisting cations (i.e., K+, Ca2+, and Mg2+). Competitive absorption behaviours under various systems showed binding strength of P-PVA in the order Pb2+ > Cd2 + > Cu2 +. The absorption mechanism of heavy metal ions was mainly governed by the complexation reaction between the phosphate functional group of P-PVA and heavy metal ions. This new adsorbent has a very high potential for practical application in the treatment of acidic and complexly polluted wastewater.

Naef A. A. Qasem et al. [54] Removal of heavy metal ions from wastewater is of prime importance for a clean environment and human health. Different reported methods were devoted to heavy metal ions removal from various wastewater sources. These methods could be classified into absorption-, membrane-, chemical-, electric-, and photocatalytic-based treatments. This paper comprehensively and critically reviews and discusses these methods in terms of used agents/adsorbents, removal efficiency, operating conditions, and the pros and cons of each method. Besides, the key findings of the previous studies reported in the literature are summarized. Generally, it is noticed that most of the recent studies have focused on absorption techniques. The major obstacles of the absorption methods are the ability to remove different ion types concurrently, high retention time, and cycling stability of adsorbents. Even though the chemical and membrane methods are practical, the large-volume sludge formation and post-treatment requirements are vital issues that need to be solved for chemical techniques. Fouling and scaling inhibition could lead to further improvement in membrane separation. However, pre-treatment and periodic cleaning of membranes incur additional costs. Electrical-based methods were also reported to be efficient; however, industrial-scale separation is needed in addition to tackling the issue of large-volume sludge formation. Electric- and photocatalytic-based methods are still less mature. More attention should be drawn to using real wastewaters rather than synthetic ones when investigating heavy metals removal. Future research studies should focus on eco-friendly, cost-effective, and sustainable materials and methods.

Zhongbing Wanget al. [55] The safe treatment of heavy metals in wastewater is directly related to human health and social development. In this paper, a new type of recyclable adsorbent is synthesized through the oxidation of enhancer and modification with magnetic nanoparticles. The new adsorbent not only inherits the advantages of multiwall carbon nanotubes (6O-MWCNTs), but also exhibits a new magnetic property and further improved absorption capacity, which is conducive to the magnetic separation and recovery of heavy metals. The absorption results indicate that multiwall magnetic carbon nanotubes

Hybrid Advances 11 (2025) 100552

(6O-MWCNTs@Fe3O4) have a good performance for Pb(II) selective absorption, with a maximum absorption capacity of 215.05 mg/g, much higher than the existing absorption capacity of the same type of adsorbents. Under the action of an external magnetic field, 6O-MWCNTs@Fe3O4 that adsorbed metal ions can quickly achieve good separation from the solution. The joint characterization results of FTIR and XPS show that under the action of both coordination and electrostatic attraction, the C=O bond in the -COOH group is induced to open by the metal ions and transforms into an ionic bond, and the metal ions are stably adsorbed on the surface of 6O-MWCNTs@Fe3O4. Pb(II) has a stronger attraction than Cu(II) and Cd(II) to the lone pair of electrons in oxygen atoms to form complexes, due to the covalent index of Pb (6.41) is more larger than that of Cu (2.98) and Cd (2.71). These data provide a new type of recyclable adsorbent for the efficient treatment of heavy metal ions in wastewater and enrich relevant theoretical knowledge.

A.Y. Jassim et al.

David B. Olawade et al. [56] Heavy metal pollution is a major threat to the environment and public health, and requires effective renovation strategies. In a nanomaterial-based approach, a promising solution removes heavy metals from water sources and uses the unique properties of the nanomaterials to improve selectivity, efficiency and sustainability. Advances in the Syntheses method, surface functionalization, and integration into existing water treatment infrastructures have shown significant potential in managing the challenges of heavy metal contamination. However, several important aspects must be considered for successful implementation of nanomaterial-based renovation techniques. Compliance with environmental impact assessment and regulatory compliance is of paramount importance to mitigate potential risks and to ensure that responsible use of nanomaterials in water treatment applications is liable. Furthermore, scalability, cost-effectiveness, and integration into other renovation technologies are important considerations for practical implementations and widespread adoption of nanomaterial-based solutions. Furthermore, continuous research efforts should focus on addressing key challenges such as nanomaterial stability, durability and multifunctionality in order to improve performance and reliability in real-world environments. Collaboration with the most important stakeholders in science, industry, government agencies and local governments is essential to foster innovation, foster technology transfer, and accelerate translation of research findings into implementable solutions.

Jianzhi Wang et al. [57] Functionalized magnetic absorber acid (FMA) was used by a simple, surface less solvent one-pot approach using acid chlorine hexahydrate as reducing agent, ethylene glycol as reducing agent, ethylene glycol using ethylene glycol synthesis as electrostatic stabilization, ethylene glycol, The self-organization process of functionalized magnetic ad soldering science has been examined, and plausible mechanisms have been proposed. The resulting functionalized magnetic intake device has relatively high specific surfaces (71.6 m2 g −1), excellent magnetic properties and abundant functional groups (carboxyl groups, hydroxyl groups, hydrophobic groups). In the meantime, the resulting FMA was used to adsorb the dyes and heavy metal ions made in aqueous solutions. Here we took two typical contaminants: dyes (methylene blue (MB) and malachite green (MG)) and toxic heavy metal ions (CR(VI)) and PB(II)) as examples of organic and inorganic pollutants in environmental waters. The excellent intrinsic properties of FMA resulted in stronger absorption capabilities than fixed solid Fe3O4 absorbent for MB, MG, Cr(VI), and PB(II). In particular, the simultaneous absorption of magnetic absorption like functionalized Blum of Mg and Pb(II) was also determined in the binary system. Finally, it was shown that the resulting flower-like magnetic advertising soybeans are expected as excellent candidates for water treatment adsorbents.

Aquib Jawed et al. [58] The current study investigates the removal of Cu(II) ions from aqueous solutions by absorption via amine-modified Fe (III)-doped-ZnO-nanoparticles (FZO) pearls. The physicochemical properties of the synthesized FZO and FZO-M balls were used using field emission electron electron microscopy, energy dissive X-ray

spectroscopy, XRIDGRACTOMTRIE (XRD), Fourier transform infrared spectroscopy (FTIR) and X-ray photoelectron specifications (XPS). We investigated the effects of various absorption parameters, including pH, temperature, dosage, contact time and initial metal concentration, for removal of Cu(II) ions. The synthesized FZO and FZO-M pearls showed complete removal of Cu(II) ions from 50 ppm aqueous solutions with doses of 1 g/L, pH, temperature at 25 °C within 720 min. Cu(II) and FZO-M-Kügelchen via FZO and FZO-M-Kügelchen were achieved as seen from the FTIR, XRD, and XPS analyses. The kinetics of Cu(II) absorption through both synthetic pearls follows the model in pseudo seconds and order, which are faster for FZO-M pearls than for FZO pearls. According to the amino modification of FZO-NPS, the maximum absorption capacity of FZO-M balls for the removal of Cu(II) ions was improved by 1.7 times and estimated at 21.5 mg/g according to the Langmuir isothermal model. The Cu(II)-D removal mechanism identified by XPS analysis showed absorption, complexation and copper oxide formation.

De Araujo et al. [59] Using the PCM/COSMO approach, the relative stability of radicals derived from anti-malarial artemisinin was calculated. Calculations were performed with polar (water) and apolar (THF) solvents at density functional levels [B3LYP/6-31G(D)]. Relative stability was calculated as a reference using isotype equations using artemisinin. It was found that substitution of oxygen atoms reduces the relative stability of the anionic radical intermediates by the CH2 unit. The degree of destabilization decreases in the presence of solvent and is less water than THF. The dipole moment and the energy without this type of corresponding solvent solution modulate this effect. Derivatives with rectangular stereochemistry are more stable than those with artemisinin-like stereochemistry, although the solvent reduces this stabilizing effect. As found in vacuo calculations, carbon-centered radicals are always more stable than their corresponding oxygen-centered radicals.

In this article, we worked on the removal of heavy metal ions from aqua solutions using graphene oxide and the modification of graphene oxide in the presence of two amines in our laboratory. Introducing amine groups to the graphene oxide surface through imitation process can significantly increase the absorption capacity of graphene oxide for heavy metal ions removal.

## 2. Materials and methods

All solvents, chemicals, and heavy metals nitrates used in this study including deionized water (DW), 30 % solution of hydrogen peroxide  $\rm H_2O_2$ , KMnO<sub>4</sub>,  $\rm H_2SO_4$ , NaNO<sub>3</sub>, HCl (5 %), tetrahydrofuran (THF), dimethylformamide (DMF), thionyl chloride (SOCl<sub>2</sub>), hydrochloric acid, ethylenediamine, dimethylformamide, carboxylic acid (R–COOH), Cu (NO<sub>3</sub>)<sub>2</sub>, Cd (NO<sub>3</sub>)<sub>2</sub>, and Pb (NO<sub>3</sub>)<sub>2</sub> were provided by Merck Co. (Germany), except for 6-aminouracil purchased from Sigma-Aldrich (France). All chemicals purchased were used as-received without further purification.

2D GO nanoparticles were synthesized using Hummers method through graphite oxidation with the aid KMnO<sub>4</sub> [21]. The procedure used was as follows: 3 g of graphite and 1.5 g of NaNO3 were poured at room temperature into a round-bottom flask, followed by the addition of 70 mL of concentrated  $H_2SO_4$  (98 %) and then cooling the mixture down to 0 °C under a water bath; after 15 min, 9 g of KMnO<sub>4</sub> was added slowly to the solution under a well-controlled condition such that the temperature of suspension remained low enough, below 20 °C. The reactants continuously stirred for 24 h in the presence of ice water bath at 0 °C; after 24 h of stirring, a thick gray paste was obtained. Then, 270 mL of DW was added to the pasty material under continuously stirring for 15 min; then 20 mL of 30 %  $\rm H_2O_2$  was slowly added, and then 60 mL of HCL (5 %) was added to the mixture, and then 30 mL of DW was again added. The color of the solution changed from brown to yellow after stirring continued for 2 days, and after that, the solution was repeatedly filtered and washed in order to make separated the acid. The mixture was centrifuged to neutralize its pH, followed by dehumidification and

drying in an oven for 24 h, ended in collecting GO nanoparticles (Fig. 3, Top) [22]. The obtained product is used for the next reaction in order to prepare 6-aminouracil and ethylenediamine functionalized GO, hereafter referred to as of GO-A and GO-E, respectively.

Functionalization of GO with 6-aminouracil precursor to gain GO-A was carried out by putting 0.5 g of GO under reflux with 20 mL of SOCl<sub>2</sub> in the presence of 0.5 mL of DMF for 24 h at 70 °C to convert the  $\rm C_2H_5OH$  attached to the surface into acyl chlorides. After refluxing, the material was dried with a rotary and placed in an oven for 24 h at 60 °C, and 20 mL of dry THF was dispersed into the resulting solid material, and then 0.5 g of 6-aminouracil was added to it and refluxed again for 24 h at 75 °C, then dried with a rotary and washed several times with DW and subsequently three times washing with ethanol. This procedure was repeated until the it was dried completely, then the materials was placed in an oven at 60 °C for 24 h until the dry amine-functionalized precursor GO-A was stored (Fig. 3, Bottom Left) [23].

Amine functionalization of GO with ethylenediamine to gain GO-E was initiated by putting 0.5 g of GO under reflux with 20 mL of SOCl<sub>2</sub> and 1 mL of DMF for 24 h at 70 °C. After refluxing, the material was dried with a rotary. The resulting product was treated with 50 mL of THF to remove the unreacted SOCl<sub>2</sub> and poured into a test tube adding 10 mL of THF and centrifuged two times and then putting the product under vacuum at 60 °C for 24 h. After drying, we took 0.5 g of the obtained product, refluxed it with 50 mL of ethylenediamine for 2 days at 100 °C, followed by filtering, washing for three times with DW and then washing it five times with pure ethanol, drying and collecting (Fig. 3, Bottom Right) [24].

Chemical structures of the synthesized GO, GO-A, and GO-E were characterized on a FTIR instrument (Spectrum Two, PerkinElmer Inc., Boston, MA). FTIR spectra were collected using a KBr pellet in a transmission mode within the wavelength of 4000-400 cm<sup>-1</sup> with spectral resolution of 4 cm<sup>-1</sup>. The structure and surface characteristics of the synthesized GO, GO-A, and GO-E were studied by a diffractometer (X Pert pro, PANalytical, Netherlands). XRD using CuKα radiation (voltage 30 kV, current 15 mA). The diffractograms were recorded with a step degree of 0.02°, with acquisition time of 2 s, and for 2 angles ranging from 10 to 60°. The morphology and the physicochemical interactions and absorptions of the GO, GO-A, and GO-E were observed in SEM images provided from GO, GO-A, and GO-E dispersions. GO, GO-A, and GO-E were dispersed within the ethanol under 15-30 min of sonication and depending on homogeneity, then a drop of the obtained suspension was placed on a graphite-coated SEM grid, dried in order to evaporate the solvent and examined by SEM (Sigma VP apparatus, Germany) at room temperature under 100 kV voltage.

As practiced in and learned from our previous works [25,27], selecting the best method for the removal of heavy metal ions from

wastewater depends on several key factors, including the initial concentration of the metal ions, and preferably the estimated cost of the operation. Moreover, chemicals added, ions removed, and their implicit environmental impacts as well as the efficacy and financial viability have to be considered. The absorption treatments used was also dependent on the absorbents.

#### 3. Results and discussion

In Fig. 4, FT-IR spectrum of GO shows a broad band at 1250 cm<sup>-1</sup>, which is attributed to the vibration of surface hydroxyl groups or vibration of surface hydroxyl groups (~3400 cm<sup>-1</sup>). In addition, the bands related to other vibrations are: C=O(-COOH) vibration (~1719 cm<sup>-1</sup>), OH deformation (~1339 cm<sup>-1</sup>), and C-O(alkoxy) and C-O(epoxy) (~1039 cm<sup>-1</sup>) stretching modes are visible at1719,1339, 1217, and 1031 cm<sup>-1</sup>. The band at 1619 cm<sup>-1</sup> can be attributed to the stretching vibrations of the C=C double bond type, and the spectra of other derivatives are also shown in Figs. 7–8. In the spectrum of 6-aminouracil and ethylenediamine, two separate spectra in the region of (~2800 cm<sup>-1</sup>) indicate the presence of –NH and –NH<sub>2</sub> groups on the GO surface.

Fig. 5 shows the small-wavelength XRD spectra of GO structure taken from the powder sample in order to estimate the amount and degree of diffraction using the relative intensity of the peaks. The presence of the intense and sharp peak at  $2\theta=8.1^\circ$  corresponds to the interplanar spacing of GO sheets. This value is attributed to a diffraction (001), which is representative of dependency on the type and the method of synthesis, as well as the number of layers of water in the interlayer space. Moreover, XRD spectrum analysis shows that the diffraction pattern corresponds to a layered structure. A comparison between XRD patterns of graphite and GO can also be seen in long-wavelength interval patterned in Fig. 6, where difference between characteristic peaks are indicative of successful formation of GO from graphite, in terms of crystallinity evolution.

The SEM image of GO platelets synthesized in this work can be seen in Fig. 7. The SEM images provided in this figure are taken from different zones and domains observed through the microscope lens and with different magnifications, which are representative of the topology of GO or the surface morphology. Such a multiplicity of spot scanning by the microscope is a measure of taking a full picture of the microstructure and topology of GO platelets. The images clearly display that the layers of GO are formed, along with its derivatives are observed clearly. In other words, these detailed and multi-spot SEM micrographs are indicative of the formation of a multi-layered nanostructure.

It was believed that surface functionalization should change such a morphology, which was assessed by SEM micrographs of GO-A and GO-E. The left-hand side column in Fig. 8 shows the SEM image of GO-A

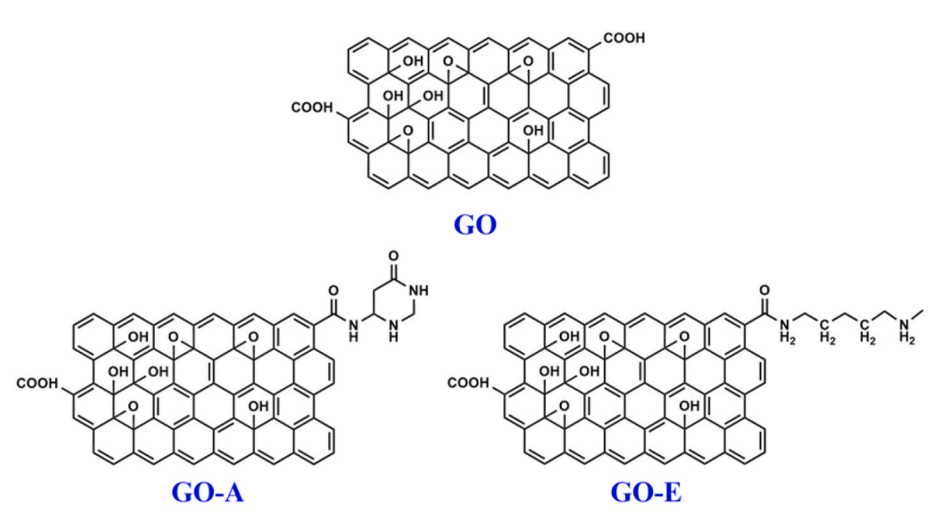


Fig. 3. Schematic chemical structures of GO (Top), and (Bottom Left), and heavy (Bottom Right) synthesized in this study [22-24].

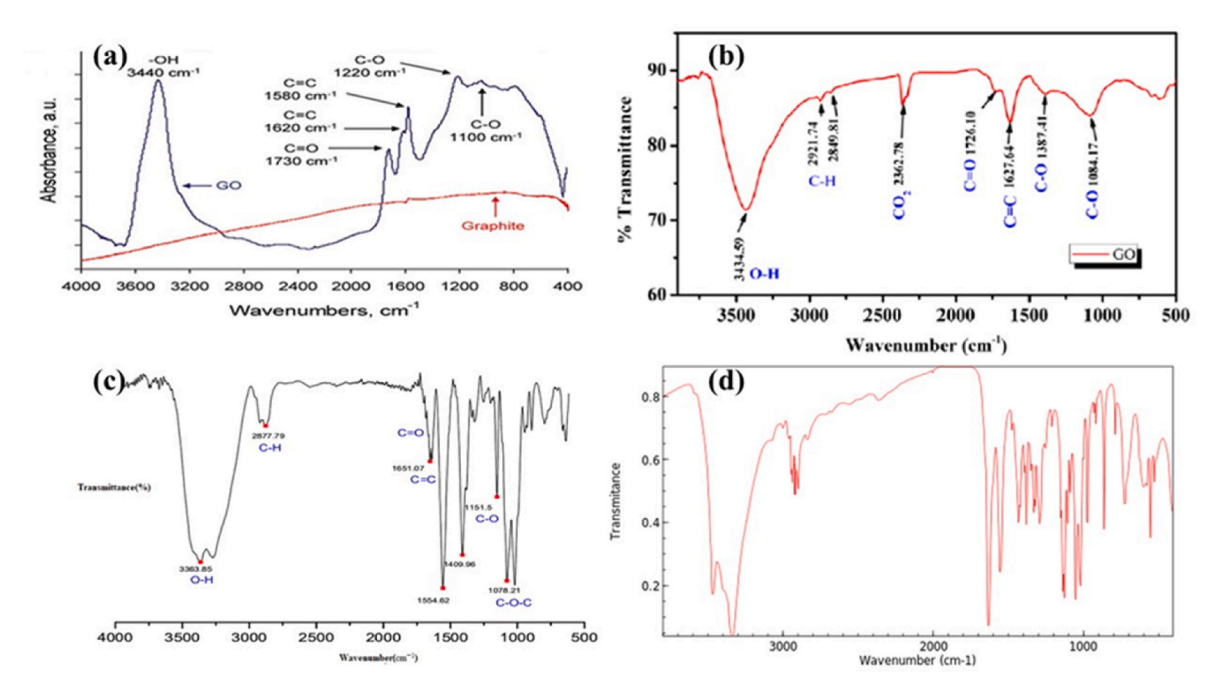


Fig. 4. FTIR spectra of graphite (a), GO (b), GO-A (c), and GO-E (d).

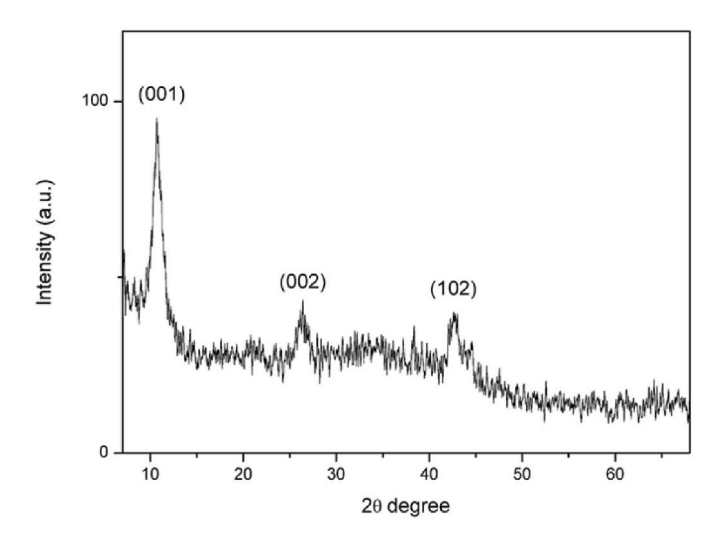


Fig. 5. Small angle XRD spectrum of GO, synthesized in this study.

carbon nanostructures prepared in this work from GO platelets through surface modification with 6-aminouracil precursor. The right-hand side column in Fig. 8 shows SEM micrographs taken from GO-E nanoplatelets, which are resulting from surface functionalization of GO with ethylenediamine. These nanostructures are synthesized with the aim that they should present a good performance in heavy metal removal from aqueous environment due to their excellent surface absorption properties originating from a hydrophilic surface with chelating groups.

There is a clue that GO nanoplatelets are partially potent to adsorb heavy metal ions distributed within an aqueous medium. The hydrophilic character as all as the abundance of functional groups such as hydroxyl and carboxyl in GO-A and GO-E nanostructures supports removal of heavy metal ions from wastewater. In this article, the aim was to improve the bonding performance between the GO nanoplatelets and pollutants, which were heavy metal ions, by the aid of two types of amines in a comparative manner. Addition of amine to GO creates an amide, and the graphene is somehow optimized and creates a compound with higher properties for adsorbing heavy metal ions at room temperature. Metal ions absorption can be in the form of physical absorption (based on electrostatic interactions) or chemical absorption (based on chemical binding). Chemical and electrostatic absorptions are combinatorial modes of absorption process. Another important factor is the presence of functional groups on the surface and surface density factor of

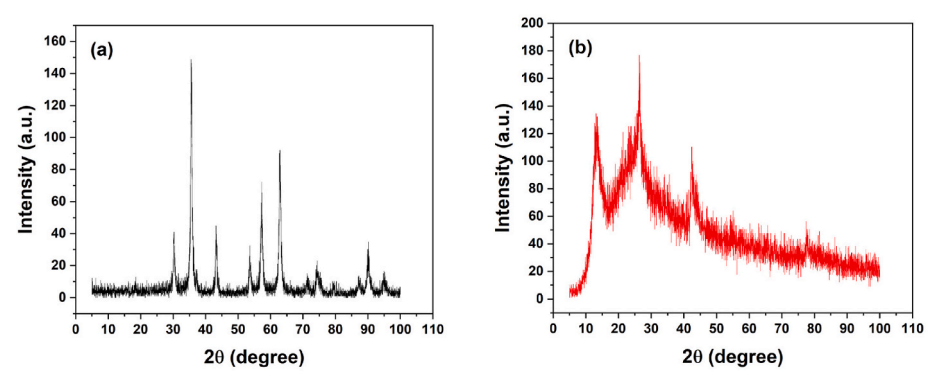


Fig. 6. Long-wavelength XRD spectra of graphite (a) and GO (b), synthesized in this study.

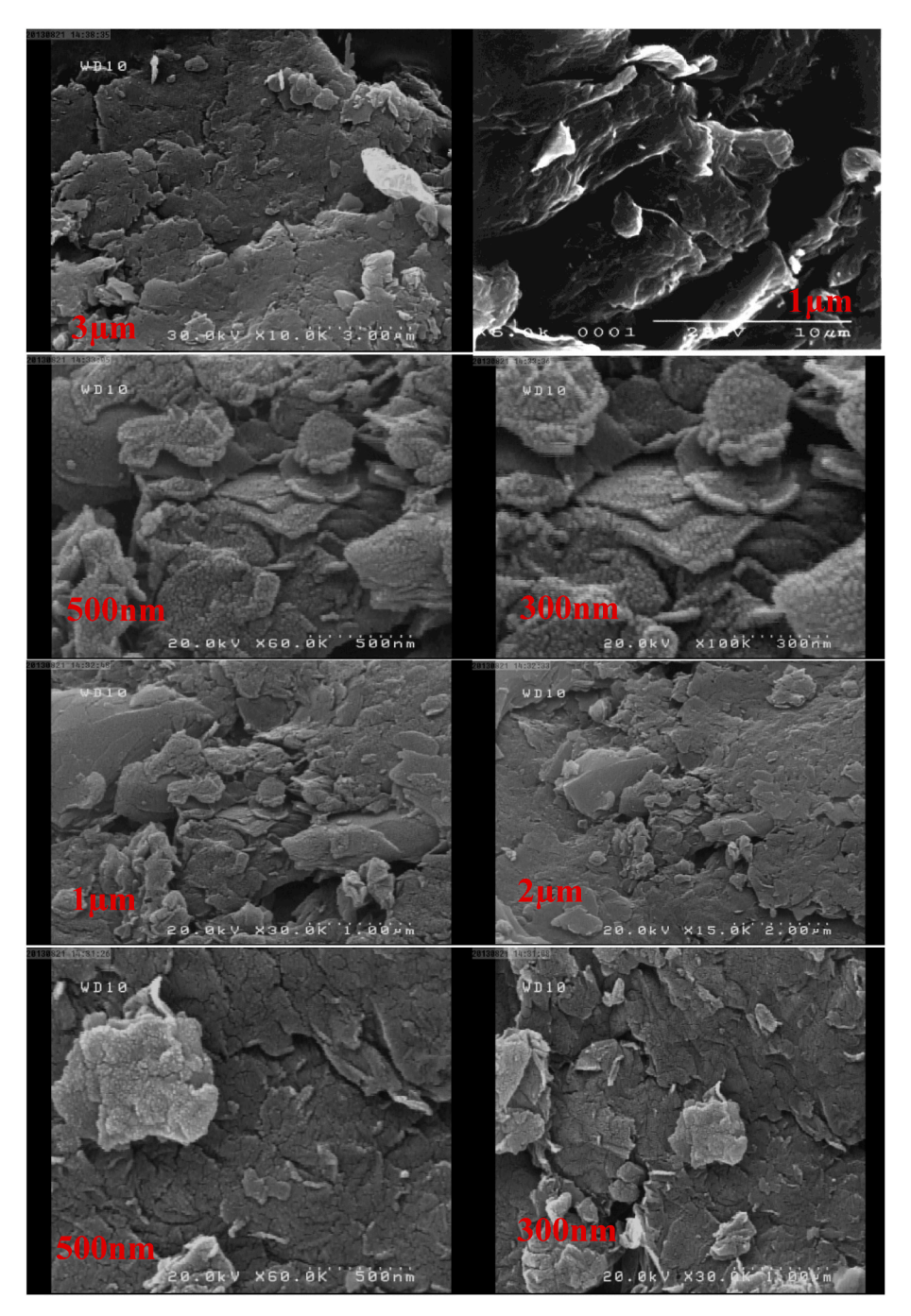


Fig. 7. SEM micrographs of GO nano-platelets provided from different spots seen through the lens of microscope.

surface groups such as carboxylic acids, hydroxyls and other groups on the surface. On the other hand, graphite oxidation leads to the creation of hydrophilic sites on the graphene structure that increase the absorption capacity of graphene. In this article, it is shown that GO and its derivatives, i.e. GO-A and GO-E are ideal absorbents for the removal of heavy metal ions from aqueous wastewater. Since the absorption capacity of carbonaceous absorbents mainly depends on the number or population of the functional groups anchored to the surface of nanostructures, the more these groups are, the more would be the contribution of absorption to heavy metal removal. When graphene is oxidized by a strong oxidant, functional groups such as carboxylic acid, hydroxyl and epoxide are formed on the surface of graphene leading to GO becoming hydrophilic. When GO is converted into its chloride compound in the presence of SOCl<sub>2</sub>, it can form a number of amide groups on

the surface of GO nanoplatelets (Equation (1)). Therefore, chelating groups are placed on the surface of GO.

$$\begin{array}{c|c} \text{GO+Socl}_2 & \xrightarrow{\text{DMF}} & \overset{\text{O}}{\text{GOC-Cl}} & \xrightarrow{\text{RNH}_2} & \text{GO-C-NH}_2 \\ & & & & & & & & & & & & & & \\ & & & & & & & & & & & \\ & & & & & & & & & & & \\ & & & & & & & & & & \\ & & & & & & & & & & \\ & & & & & & & & & & \\ & & & & & & & & & \\ & & & & & & & & & \\ & & & & & & & & \\ & & & & & & & & \\ & & & & & & & & \\ & & & & & & & & \\ & & & & & & & \\ & & & & & & & \\ & & & & & & & \\ & & & & & & & \\ & & & & & & & \\ & & & & & \\ & & & & & \\ & & & & & \\ & & & & & \\ & & & & & \\ & & & & & \\ & & & & & \\ & & & & \\ & & & & & \\ & & & & \\ & & & & \\ & & & & \\ & & & & \\ & & & & \\ & & & & \\ & & & & \\ & & & & \\ & & & & \\ & & \\ & & & \\ & & \\ & & \\ & & \\ & & & \\ & \\ & & \\ & & \\ & & \\ & & \\ & & \\ & & \\ & & \\ & & \\ & & \\ & & \\ & &$$

Two absorption processes are responsible for the absorption of heavy metal ions by the GO surface or absorbents; ion exchange reaction between metal ions and carboxyl groups (COOH-) or hydroxyl groups (OH-) and surface complexation. The second process of metal ion complexation with amine functional groups, the first absorption mechanism is an ion exchange reaction between metal ion and COOH- and OH- groups.

Mechanism (I): Heavy metal ion reacts with COOH- and OH- groups

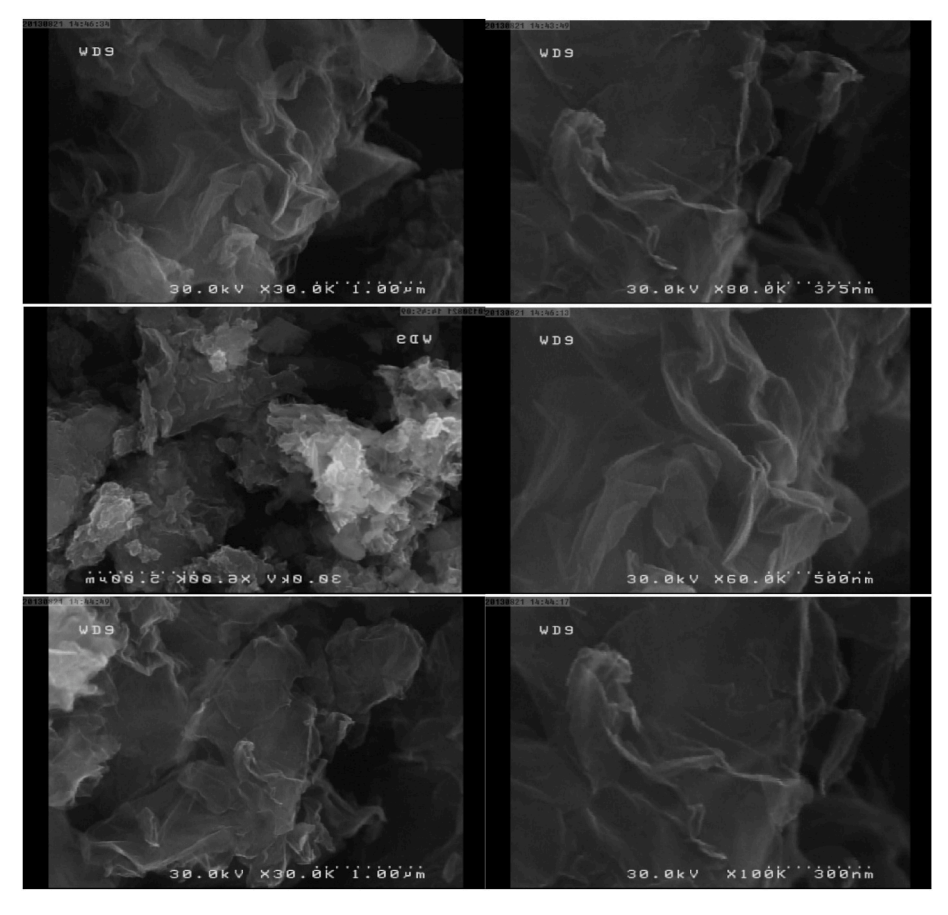


Fig. 8. SEM micrographs of GO-A (left-hand side column) and GO-E (right-hand side column) nano-platelets provided from different spots seen through the lens of microscope.

on the surface of GO and forms a complex, as follows:

$$\begin{aligned} & \text{GO-COOH} + \text{M}^{2+} \!\rightarrow\! \text{GO-COO}^{\text{-}} \! \text{M}^{2+} + \text{H}^{+} \\ & (\text{GO-COOH})_{2} + \text{M}^{2+} \!\rightarrow\! (\text{GO-COO})^{\text{-}} \! \text{M}^{2+} + 2\text{H}^{+} \\ & \text{GO-OH} + \text{M}^{2+} \!\rightarrow\! \text{GO-O}^{\text{-}} \! \text{M}^{2+} + 2\text{H}^{+} \\ & (\text{GO-OH})_{2} + \text{M}^{2+} \!\rightarrow\! (\text{GO-O})^{\text{-}} \! \text{M}^{2+} + 2\text{H}^{+} \end{aligned} \tag{2}$$

Mechanism (II): The reaction is between metal ions and functional groups on the GO surface, as follows.

O 
$$\parallel$$
 GO-CNHCH<sub>2</sub>CH<sub>2</sub>NH+M<sup>2+</sup>  $\longrightarrow$  GO-NHCH<sub>2</sub>CH<sub>2</sub>NH<sub>2</sub>  $\stackrel{\wedge}{M^{2+}}$ 

Graphene oxide is optimized by 6-aminouracil diethylenediamine and studied in the process of absorption and separation of heavy metal ions. Graphene oxide partially has the ability to absorption metal ions in aqueous medium. The hydrophilic character and the presence of functional groups such as hydroxyl and carboxyl help to remove metal ions. In this article, the aim is to improve the bonding properties of graphene oxide by two types of amines. Addition of amine to graphene oxide creates an amide, and the graphene is somehow optimized and creates a compound with better properties for absorbing metal ions at room temperature. Metal ions absorption on the absorption can be in the form of physical absorption (based on electrostatic interactions) or chemical absorption. Chemical and electrostatic absorption are two important and influential factors in the absorption process (Fig. 9).

With the absorption of heavy metal ions on the surface of GO nanoplatelets, the pH of the environment becomes acidic, and due to the

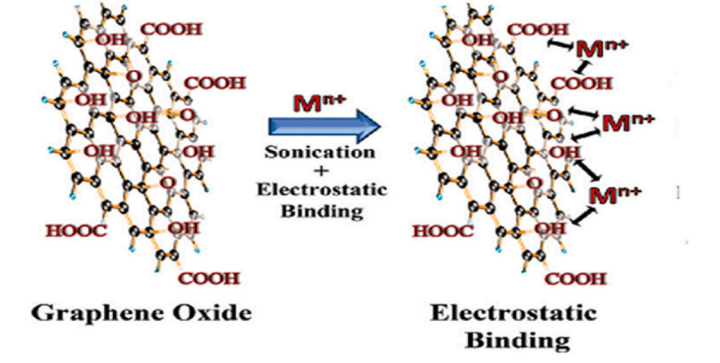
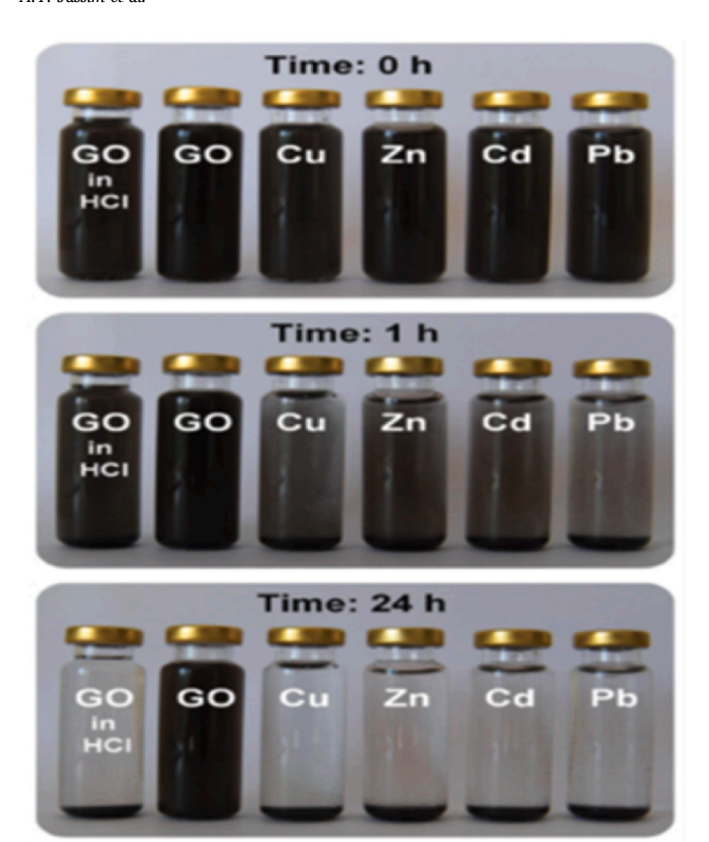


Fig. 9. Absorption of metal ions by electrostatic interactions on GO surface.

formation of complexes between heavy metal ions and functional groups, more stable structures must be formed. This is a kind of emphasis to increase the absorption capacity of the absorption. Fig. 10 shows digital image of the absorption of heavy metal ions by the absorbent. For a comprehensive review of the absorption process and the influencing factors, the effects of the amount of absorbent and the concentration time of the pollutants are further investigated.

The absorption behavior of heavy metal ions is related to the contact time. In the study, it was proved that the change of time from 5 min to 60 min affects the amount of absorption. The amount of copper ion  $(\text{Cu}^{2+})$  absorption on each of the absorbents has been monitored at different times and the desired absorbent amount of 2 mg has been measured at room temperature. The results are reported in Fig. 11a. The amount of cadmium ion  $(\text{Cd}^{2+})$  absorption on each of the absorbents has

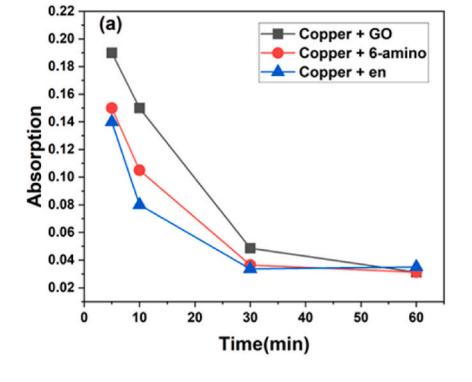


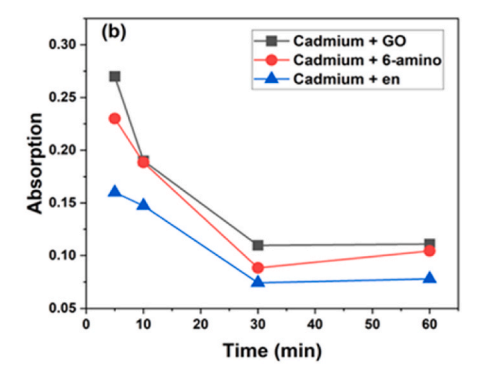
**Fig. 10.** Digital photos of heavy metals absorption by GO and its derivatives as a function of time.

also been monitored as a function of time under constant absorbent amount of 2 mg for the sake of comparison at room temperature, and the results are reported in Fig. 11b. The amount of lid ion (Pb $^{2+}$ ) absorption on each of the absorbents has similarly been measured at different times under desired absorbent amount of 2 mg at room temperature, and the results are reported in Fig. 11c. Overall, descending trend over time was expectedly seen regardless of adsorbent type, but the presence of 6-aminouracil and ethylenediamine groups, respectively in GO-A and GO-E nanosheets, slowed down the absorption process, a characteristic of higher efficiency and more surface contribution from the adsorbent to the pollutants.

The absorption behavior of three absorbents of GO, GO-A, and GO-E nanosheets was captured as a responding variable in terms of the amounts of GO, GO-A, and GO-E as of 0.5, 1, 2, and 5 mg at a constant time of 30 min for copper metal ions. The results are shown in Fig. 12. As the results confirm, the amount of 2 mg of absorption is optimal, such that the curves leveled off at that concentration.

The behavior of absorption by the aid of GO, GO-A, and GO-E nanosheets used as absorbents at constant concentration of 2 mg and varying pH of the simulated wastewater has been plotted for three types of heavy metal ions, as presented in Fig. 13. Overall, it is observed that acidic solutions undergone higher absorption efficiency, which is the case for such pollutants. On the other hands, the selectivity of absorbents towards heavy metal ions should be taken into account. This is an indication of the role of surface functional groups on the selectivity of absorption depending on the type of pollutant. For instance, Cu<sup>2+</sup> has been adsorbed by the absorbents (Fig. 13a) following an efficiency in the order of GO > GO-A > GO-E. On the other hands,  $Cd^{2+}$  could be removed from wastewater more easily and efficiently by the GO-E, such that absorbents were successful in Cd<sup>2+</sup> removal in the order of GO-E > GO-A > GO (Fig. 12), which is in vivid contradiction with removal of Cu<sup>2+</sup>. The equilibrium state was indeed achieved more quickly in highly acidic wastewater solutions, but surface functionality of absorbents





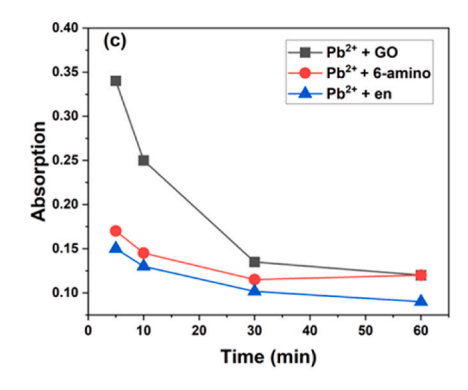


Fig. 11. The variation of absorption rate for  $Cu^{2+}$  (a),  $Cd^{2+}$  (b), and  $Pb^{2+}$  (c) heavy metal ions as a function of absorption time under specific pollutant concentration and applying 2 mg of GO, GO-A, and GO-E absorbents at room temperature.

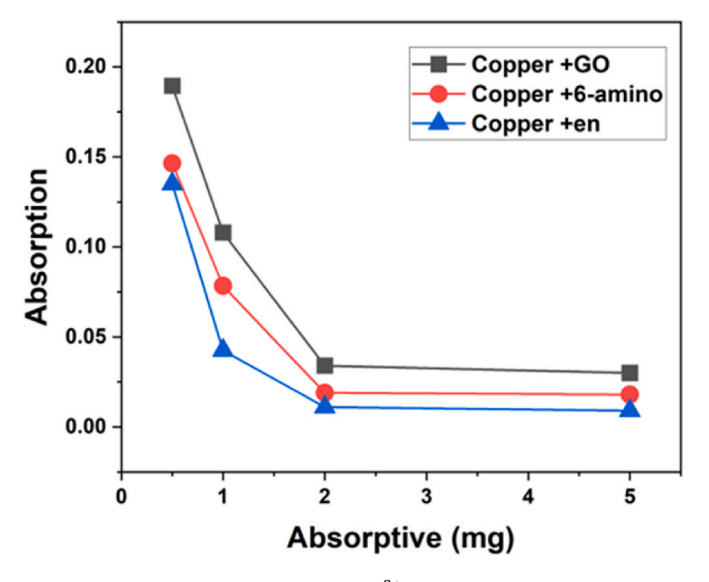


Fig. 12. The variation of absorption for  $\mathrm{Cu}^{2+}$  heavy metal ions as a function of the amount of GO, GO-A, and GO-E absorbents over 30 min absorption process at room temperature.

played as the most key parameter in absorption efficiency. Such an absorption capacity could basically affect the design and engineering of adsorbent surface chemistry, which has been systematically served and proved in this work. Another feature of this comparative analysis is the amount of pollutant adsorbed, which can be seen in the vertical axes of bar diagrams in Fig. 13. For instance, Pb<sup>2+</sup> was separated less independent from pH (Fig. 13c), but pH-dependent Cd<sup>2+</sup> removal (Fig. 13b) took higher absolute values if absorption, which are related to the functionality and chemistry of pollutants and absorbents' surface

functionality.

Nanotube Modular software was used to draw the nanostructure of graphene, while Goose view software, version 5, was used to virtually functionalize the surface of graphene and dope the polluting metals considered in the experimental section, i.e.  $Cu^{2+}$ ,  $Cd^{2+}$ , and  $Pb^{2+}$  heavy metal ions. In the computational section, which includes optimizing the Absorption - Absorption structures, the stability of the constructed structures was captured in order to determine the highest pollutant absorption rate on the graphene nano Absorption as a result of surface engineering of graphene oxides, i.e., by comparing the results of two experimental methods and quantum mechanics computations. On the other hand, there was a challenge of determining the ability of computational methods to predict the amount of absorption of pollutants on Absorption surfaces and eventually the thermodynamic properties of those structures. Calculations were carried out at the levels of density functional theory (DFT) and with the basis sets g21-3 and (p,d) g31-6 in two gas and solvent phases (the solvent used in the experiment and calculations is water) in Gossin 09 software. It is necessary to emphasize that for heavy metals, their appropriate base set, i.e., LANL2DZ, was used. The energy amounts for the compounds in the gas phase were calculated with g21-3 basis set and the stability level for all levels and heavy metal elements were checked according to Table 1.In the presence of absorbents, it can be seen that the Cu<sup>2+</sup> heavy metal ions show the highest stability than Cd<sup>2+</sup> and Pb<sup>2+</sup> heavy metal ions, obviously more than Cd2+ and Pb2+. From wastewater removal point of view, this confirms that the Cu<sup>2+</sup> heavy metal ions should be highly capable of undergoing surface absorption by various types of graphene oxides compared to Cd<sup>2+</sup> and Pb<sup>2+</sup> ions whatever surface chemistry. Moreover, the most suitable nanosheet among GO, GO-A, and GO-E three absorbents is the ethylene diamine surface functionalized GO, i. e. GO-E, which is clearly evident from the comparison of the values in Table 1. This theoretical finding is in agreement with experimental investigations on absorbent. In a similar manner, the energy values for the

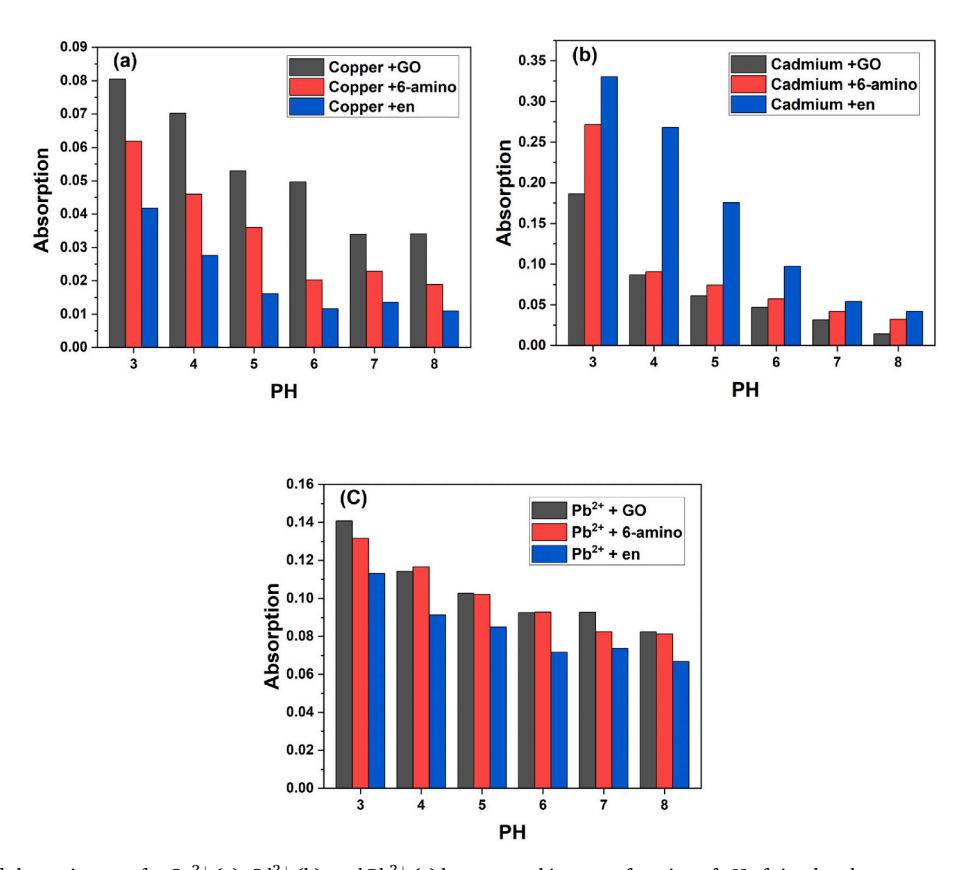


Fig. 13. The variation of absorption rate for  $Cu^{2+}$  (a),  $Cd^{2+}$  (b), and  $Pb^{2+}$  (c) heavy metal ions as a function of pH of simulated wastewater applying 2 mg of GO, GO-A, and GO-E absorbents at room temperature.

Table 1
Comparison of energy used in absorption (stability) obtained based on molecular orbital calculations between three levels and three heavy metal ions in the gas phase with g21-3 basis set, in the solvent phase with the g21-3 base set, and in the solvent phase with the g31-6 base set.

Surface type	Metal (Kcal.mol <sup>-1</sup> ) Energy				
	Cu <sup>+2</sup>	Cd <sup>+2</sup>	Pb <sup>+2</sup>		
Gas phase with g	Gas phase with g21–3 basis set.				
GO	-422.640	-303.8945	-268.654527		
GO-A	-430.8218	-320.8399	287.4874327		
GO-E	-494.2153	-330.1084	-289.27133		
Solvent phase wi	Solvent phase with the g21-3 base set.				
GO	-127.4306	-50.43120	-24.32102		
GO-A	-185.8205	-51.6272	-25.31341		
GO-E	-234.7327	-55.96914	-27.45224		
Solvent phase with the basis set (p,d) g31-6.					
GO	-146.4201	-58.3210	-38.25702		
GO-A	-198.4231	-62.4371	-40.2351		
GO-E	-275.64302	-72.3041	-41.3302		

 $1 \text{hartree} = 627.51 \text{ kcal mol}^{-1}$ 

 $\Delta E_{Total} = \Delta E_{Metal} + N_{ano} - (\Delta E_{Metal} + \Delta E_{Nano}).$ 

compounds in the solvent phase calculated with the g21-3 basis set are voting for the highest stability level for all kinds of surfaces and heavy elements was reported according to Table 1. In the presence of absorbents, it is observed that  $\text{Cu}^{2+}$  serves the highest stability than other heavy metal ions. This means that  $\text{Cu}^{2+}$  should be more capable of being adsorbed on the surface of various types of nanosheets than  $\text{Cd}^{2+}$  and  $\text{Pb}^{2+}$ . Likewise, GO-E appeared as the most suitable nanosheet adsorbent among the three used, which is crystal clear from the comparison of the values in Table 1. For the solvent phase analysis carried out theoretically with the g21-3 base set, the amount of metal settling on the ethylene diamine absorbent is the most intense taking the highest surface absorption. According to Table 1, the energy values for compounds in the solvent phase were calculated with the basis set (p,d) g31-6 and the stability level for all surfaces and heavy metal elements were computed.

Overall, it can be concluded that the Cu<sup>2+</sup> heavy metal ion takes the highest stability in terms of absorption energy in the presence of absorbents than the other heavy metals. This means that the Cu<sup>2+</sup> ion should be highly capable of experiencing surface absorption by all kinds of nanosheets than Cd<sup>2+</sup> and Pb<sup>2+</sup>. The most suitable nanosheet among the three-surface engineered graphemic absorbents is the one surface functionalized with ethylene diamine, which is GO-E with clearly higher negative energy values compared to the GO and GO-A, evident from Table 1. In the case of solvent phase on the bedrock of the base set (p,d) g31-6, for the Cu<sup>2+</sup> heavy metal ions the amount of metal sitting on the ethylene diamine functionalized absorbent (GO-E) is the highest, but this trend is more intense for the Cu<sup>2+</sup> heavy metal ion in the presence of the GO-E absorbent. To have a wider image of theoretical investigation, enthalpy and Gibbs free energy computations are frequently recommended.

Calculation of theoretical enthalpy values in the gas and solvent phases is reported for g21-3 basis set and for solvent phase (solvent is same as water experimental method) with (p,d)g31-6 basis set, respectively. According to Table 2, from the comparison of the gas phase results in the vicinity of GO, GO-A, and GO-E nanosheet absorbent surfaces, it can be inferred that the interaction between ethylenediamine from GO-E and Cu<sup>2+</sup> heavy metal ion is extremely exothermic. Therefore, this adsorbent can easily adsorb Cu<sup>2+</sup> heavy metal ion from industrial wastewater, which agrees well with experimental analysis. By comparing the computational results of the gas phase and the solvent phase with the g21-3 base set, it can be concluded that the solvent phase has a greater tendency towards the absorbent than the gas phase, and definitely such a tendency is more with GO-E bearing ethylenediamine on its surface. From the comparison of the results of the solvent phase for

Table 2
Comparison of the enthalpy of absorption reaction obtained based on molecular orbital calculations between three levels and three metal ions in the gas phase with g21-3 basis set, in the solvent phase with the g21-3 base set, and in the solvent phase with the g31-6 base set.

Surface type	Metal (Kcal.mol <sup>-1</sup> ) Energy			
Gas phase with	g21–3 basis set.			
GO	-422.640	-303.8945	-268.654527	
GO-A	-430.8218	-320.8399	287.4874327	
GO-E	-494.2153	-330.1084	-289.27133	
Solvent phase w	Solvent phase with the g21-3 base set.			
GO	-127.4306	-50.43120	-24.32102	
GO-A	-185.8205	-51.6272	-25.31341	
GO-E	-234.7327	-55.96914	-27.45224	
Solvent phase w	ith the basis set (p,d)	g31-6.		
GO	-146.4201	-58.3210	-38.25702	
GO-A	-198.4231	-62.4371	-40.2351	
GO-E	-275.64302	-72.3041	-41.3302	

 $1 \text{hartree} = 627.51 \text{ kcal mol}^{-1}$ 

 $\Delta E_{Total} = \Delta E_{Metal} + {}_{Nano}\text{-}(\Delta E_{Metal} + \Delta E_{Nano})\text{.}$ 

the two basic sets g21-3 and (p,d)g31-6, again GO-E follows a significantly exothermic reaction. Thus, Cu<sup>2+</sup> heavy metal ion among the phases and the set bases show better results in the solvent phase with the (p,d)g31-6 basis set. For Cd<sup>2+</sup>, according to Table 2, computations resulted in very similar values in the gas phase and in the solvent phase (with two basis sets g21-3 and (p,d)g31-6). This is while  $Cu^{2+}$  absorption levels differ from each other in all phases, characteristic of the impact of surface functionalization of GO on removal efficiency of Cu<sup>2+</sup> pollutants. For the Pb<sup>2+</sup> heavy metal ion, the highest heat of reaction has been achieved in the gas phase with g21-3 basis set, which is comparable with those of Cu<sup>2+</sup> and Cd<sup>2+</sup>. This means that absorption is neither highly pollutant dependent nor surface chemistry dependent in the gas phase. On the other hand, both surface chemistry and pollutant type pose a great influence of the enthalpy of absorption reaction in the solvent phase either the g21-3 base set or solvent phase with the basis set (p,d) g31-6. This finding is of elegant important in design and application of GO-based absorbents, where the surface chemistry plays a key role in determining both the quality and quantity of heavy metal ions' absorption.

Calculation of Gibbs free energy in gas and solvent phases is reported for g21-3 basis set and for solvent phase (water solvent is same as experimental method) with (p,d) g31-6 basis set. According to Table 3, from the comparison of the gas phase results in the vicinity of GO, GO-A, and GO-E, one can conclude that the reaction of ethylenediamine compound present on the surface of GO-E with Cu<sup>2+</sup> heavy metal ion is highly spontaneous (more tendency for surface absorption), therefore, one could expect rapid and more likely absorption of Cu<sup>2+</sup> heavy metal ion on the surface of GO-E compared to GO and GO-A. By comparing the results of the gas phase and the solvent phase with the g21-3 base set, it appears crystal clear that absorption is obviously both pollutant- and adsorbent dependent, but in each phase the dependency to pollutant is highly touchable. Moreover, although absolute values are vividly higher in the gas phase, absorption in the solvent phase is more pollutant dependent that the gas phase. Evidently, the theoretical values of Gibbs free energy obtained for Cu<sup>2+</sup>, Cd<sup>2+</sup>, and Pb<sup>2+</sup> obviously differ from each other between two to three times, demonstrating higher efficiency of absorption towards Cu<sup>2+</sup> heavy metal ions. It is also worth mentioning that absorption tendency is stronger for ethylenediamine functionalized GO-E adsorbent. From the comparison of the results of the solvent phase for the two basic sets g21-3 and (p,d)g31-6, again the result for the GO-E are remarkably notifying a spontaneous reaction. This means that the Cu<sup>2+</sup> heavy metal ion can be removed easily by this series of nanosheet absorbents. The bases show better results in the

**Table 3**Comparison of the values of Gibbs free energy obtained based on molecular orbital calculations between three levels and three metal ions in the gas phase with g21-3 basis set, in the solvent phase with the g21-3 base set, and in the solvent phase with the g31-6 base set.

Surface type	Metal (Kcal.mol <sup>-1</sup> ) Energy				
	Cu <sup>+2</sup>	Cd <sup>+2</sup>	Pb <sup>+2</sup>		
Gas phase with g	Gas phase with g21–3 basis set.				
GO	-422.640	-303.8945	-268.654527		
GO-A	-430.8218	-320.8399	287.4874327		
GO-E	-494.2153	-330.1084	-289.27133		
Solvent phase with the g21-3 base set.					
GO	-127.4306	-50.43120	-24.32102		
GO-A	-185.8205	-51.6272	-25.31341		
GO-E	-234.7327	-55.96914	-27.45224		
Solvent phase with the basis set (p,d) g31-6.					
GO	-146.4201	-58.3210	-38.25702		
GO-A	-198.4231	-62.4371	-40.2351		
GO-E	-275.64302	-72.3041	-41.3302		

 $1 \text{hartree} = 627.51 \text{ kcal mol}^{-1}$ 

 $\Delta E_{Total} = \Delta E_{Metal} + N_{ano} - (\Delta E_{Metal} + \Delta E_{Nano})$ .

solvent phase with the (p,d)g31-6 basis set. According to Table 3,  $Cd^{2+}$  tends to spontaneous absorption on all nanosheets more than  $Pb^{2+}$ , where again the GO-E usage leads to highly spontaneous absorption compared to GO and GO-A in both gas and solvent phases. Overall, more reactive sites of GO-A and GO-E compared to GO enhanced the probability of coordination of heavy metal ions under ambient temperature with absorbents.

Since there is more than one component in the absorption process, there should be an equilibrium and interaction between the components. The previously discussed isotherm models were for the description of mono-parametric absorption systems. Hence, studying multiparametric systems requires new absorption isotherm models to adequately represent the absorption processes. Since multi-parametric models were extrapolated from the mono-parametric isotherm models, so their classification is based on the models they were extended from Ref. [47]. Various multi-parametric absorption isotherm models are illustrated in Table 4.

Therefore, recycling, detection and removal of these heavy metals is important from both environmental and economic perspectives, especially in the case of toxic metals. Recently, various technologies such as ion exchange, chemical deposition, evaporation, absorption, reverse osmosis and electrochemistry have been used to separate heavy metal ions. There are limitations in using these methods such as low selectivity, low capacity to collect metal ions and produce other toxic compounds [25–28]. Despite these shortcomings, the efficiency of these methods is important from an economic point of view, and this efficiency and their application depends on the affinity between the adsorbent and the target pollutants. Some common heavy metals such as cadmium, zinc and copper sources and its effect on human health are mentioned in Table 5.

### 4. Conclusion

Graphene oxide (GO) has been chosen as a carbon-based adsorbent and by functionalization of its surface a series of nanosheet absorbents synthesized, characterized, and out in competition in absorption of heavy metal ions from wastewater solutions. The role of surface chemistry of this series of absorbents for the absorption of heavy metal ions in the form of non-covalent interactions (non-bonded and van der Waals) as well as bonded interactions (Covalent bond) were evaluated both experimentally and theoretically. Two amine groups, one linear amine and the other a cyclic amine were attached to the surface of GO, which significantly improved the absorption of heavy metal ions by the

**Table 4**Description of absorption isotherm models that are used for multi-parametric systems.

Absorption isotherm model	Description	Ref
Extended Langmuir multi- parametric isotherm	<ul> <li>It assumes that there is a similarity between all the present active sites on the adsorbent surface, and there is equal competition between the species present in the environment for the same active sites.</li> <li>With respect to the mono-parametric system, the precision of the obtained values is more when it is closer to the species absorption capacity values.</li> <li>Similarly, to the EL model, it assumes the similarity between the active sites and species compete equally for the same active sites.</li> </ul>	[48]
Non-modified Langmuir (N-ML) model	Since this model uses the mono- parametric absorption parameters, species adsorbed in multi-parametric system is not represented adequately.	[49]
Modified Langmuir isotherm (ML)	<ul> <li>It evaluates the ions' unequal competition from the adsorbent's active sites through incorporating the ηL constant parameters in its formula.</li> <li>ηL values are obtained from the multi-parametric absorption process in which its characteristic for each species.</li> </ul>	[50]
Extended selective Langmuir isotherm (ESL)	<ul> <li>It assumes that part of the adsorbent surface will be covered by each ion of the existing ions in the mixture.</li> <li>The summation of all the absorption capacities for all the species and multiplying it with the molar fraction of the adsorbed species yields the maximum absorption capacity of the adsorbent.</li> </ul>	[51]
Extended Freundlich (EF) multi- parametric isotherm	<ul> <li>Can be applied in non-ideal systems.</li> <li>Better fits of this model depend on the heterogeneity of the absorbent surfaces allowing various interaction types with the existing species in the solution.</li> </ul>	[52]
Sheindrof – rebuhn – sheintuch (SRS) isotherm	<ul> <li>It is an extension of Freundlich isotherm model.</li> <li>It considers the competition between the existing species in the absorption system and how they affect the absorption of each other.</li> <li>It assumes that there is an exponential distribution of site absorption energy of each component in the multi- parametric system.</li> </ul>	[53]
Non-modified Redlich – Peterson (N-MR-P) multi-parametric isotherms Modified Redlich – Peterson (MR-	This extended model assumes that there is an equal competition between adsorbent's active sites and the ions.  • It uses the multi-parametric compe-	[54] [55]
P) multiparametric isotherms	<ul> <li>tition constant (ηR,i) for the evaluation of unequally competitive absorption.</li> <li>Compared to competing species, the smaller the species value, the greater the affinity towards the adsorbent's active sites.</li> </ul>	
Extended sips (ES) mode	This model can only be applicable to systems that present active sites with heterogeneous energies.	[55]
Ideal absorption solution theory – sips (IASTS) model	It is applicable to absorbents with surfaces having homogenous active sites.	[55]

**Table 5** Sources and health effect of heavy metals [25–28].

Metals	Major Sources	Health effect
Cadmium	Electroplating and	Harms kidney function, Gastrointestinal
	Batteries	disorder, Bone defects (itai-itai,
		osteomalacia, osteoporosis),
		Nephrotoxicity, Anemia, Anosmia,
Cadmium	Duce and Daint mismants	Ulceration, Carcinogenesis effects
Cadmium	Dyes and Paint pigments Pesticide and Fertilizer	// //
Cadmium		
Cadilliulli	Nuclear plant and Coating operations	//
Copper	Mining Metal and	Hemodialysis (Kidney Damage), Nausea,
	Electrical manufacturing	Vomiting, Bloody diarrhea, Fever,
		Stomach pain, Low blood pressure,
		Anemia.
Copper	Agriculture and domestic	//
	pesticides and fungicides	
Copper	Finishing and Leather	//
	Processing	
Zinc	Electroplating, Smelting	Effect calcification of bone Alzheimer's
	and Mining	disease, Corrosive and harmful to the
		mucous membranes, Adverse effect on
		gastrointestinal tissue, Throat burning,
		Abdominal pain and diarrhea,
		Hematological changes, Anemia
Zinc	Rodenticides and Herbicide	//
Zinc		//
Zinc	Dyes and Paint pigments	//
ZIIIC	Wood preservative and Solubilizing agents	//
Zinc	Galvanizing agents  Galvanizing and Metal	//
ZIIIC	processing	//
	Processing	

absorbent. The results also show that the ethylenediamine group on the surface of GO-E provides a higher active surface to the pollutants in comparison with 6-aminouracil in the GO-A. It was inferred that the ethylenediamine amino group could better coordinate with metal ions, such that the number of ethylenediamine substitutions on the GO surface might have been vividly more comparatively. Since the  $\mbox{\rm Cu}^{2+}$  heavy metal ion is smaller in size and radius with respect to the Cd<sup>2+</sup> and Pb<sup>2+</sup> heavy metal ions, it could more easily provide support for surface absorption. The investigation shows that in the presence of a constant amount of absorbent at ambient temperature and pressure the rate of absorption was higher for  $\mathrm{Cu}^{+2}$  ion, as theoretically confirmed based on enthalpy and Gibbs free energy values. Overall, the theoretical results were in very good agreement with the experimental ones, such that Cu<sup>+2</sup> ion were dialed in by the ethylenediamine group in GO-E, where the reaction was highly spontaneous based on Gibbs free energy computations. Evidently, the intensity of spontaneous absorption of the absorbent on the absorbed surface was more obvious for the Cu<sup>+2</sup> ion in the case of GO-E.

## CRediT authorship contribution statement

Amar Yasser Jassim: Writing – review & editing, Writing – original draft, Methodology, Investigation. Balqees Suhaem Al-Ali: Writing – review & editing, Writing – original draft, Methodology, Investigation. Wesam R. Kadhum: Writing – review & editing, Investigation, Conceptualization. Ehsan kianfar: Writing – review & editing, Writing – original draft, Supervision, Methodology, Investigation.

## Ethics approval and consent to participate

Not applicable.

## Consent for publication

Not applicable.

#### **Funding**

Not applicable.

## **Declaration of competing interest**

The authors declare that they have no known competing financial interests or personal relationships that could have appeared to influence the work reported in this paper.

#### Data availability

All data generated or analyzed during this study are included in this published article.

#### References

- [1] Z. Nasrollahi, M.S. Hashemi, S. Bameri, V. Mohamad Taghvaee, Environmental pollution, economic growth, population, industrialization, and technology in weak and strong sustainability: using STIRPAT model, Environ. Dev. Sustain. 22 (2020) 1105–1122
- [2] S. Khalid, M. Shahid, Natasha, I. Bibi, T. Sarwar, A.H. Shah, N.K. Niazi, A review of environmental contamination and health risk assessment of wastewater use for crop irrigation with a focus on low and high-income countries, Int. J. Environ. Res. Publ. Health 15 (5) (2018) 895.
- [3] M.A. Rahman, H. Hasegawa, High levels of inorganic arsenic in rice in areas where arsenic-contaminated water is used for irrigation and cooking, Sci. Total Environ. 409 (22) (2011) 4645–4655.
- [4] Q. Zhou, N. Yang, Y. Li, B. Ren, X. Ding, H. Bian, X. Yao, Total concentrations and sources of heavy metal pollution in global river and lake water bodies from 1972 to 2017, Glob. Ecol. Conserv. 22 (2020) e00925.
- [5] V. Srivastava, A. Sarkar, S. Singh, P. Singh, A.S. De Araujo, R.P. Singh, Agroecological responses of heavy metal pollution with special emphasis on soil health and plant performances, Front. Environ. Sci. 5 (2017) 64.
- [6] U. Okereafor, M. Makhatha, L. Mekuto, N. Uche-Okereafor, T. Sebola, V. Mavumengwana, Toxic metal implications on agricultural soils, plants, animals, aquatic life and human health, Int. J. Environ. Res. Publ. Health 17 (7) (2020) 2204
- [7] M.S. Mimoto, A. Nadal, R.M. Sargis, Polluted pathways: mechanisms of metabolic disruption by endocrine disrupting chemicals, Curr. Environ. Health Rep. 4 (2017) 208, 222
- [8] A.J. Green, A. Planchart, The neurological toxicity of heavy metals: a fish perspective, Comp. Biochem. Physiol. C Toxicol. Pharmacol. 208 (2018) 12–19.
- [9] C. Nyambura, N.O. Hashim, M.W. Chege, S. Tokonami, F.W. Omonya, Cancer and non-cancer health risks from carcinogenic heavy metal exposures in underground water from Kilimambogo, Kenya, Groundwater Sustain. Dev. 10 (2020) 100315.
- [10] N. Johri, G. Jacquillet, R. Unwin, Heavy metal poisoning: the effects of cadmium on the kidney, Biometals 23 (2010) 783–792.
- [11] O. Hyder, M. Chung, D. Cosgrove, J.M. Herman, Z. Li, A. Firoozmand, T.M. Pawlik, Cadmium exposure and liver disease among US adults, J. Gastrointest. Surg. 17 (2013) 1265–1273.
- [12] S. Khalid, M. Shahid, Natasha, I. Bibi, T. Sarwar, A.H. Shah, N.K. Niazi, A review of environmental contamination and health risk assessment of wastewater use for crop irrigation with a focus on low and high-income countries, Int. J. Environ. Res. Publ. Health 15 (5) (2018) 895.
- [13] R. Shrestha, S. Ban, S. Devkota, S. Sharma, R. Joshi, A.P. Tiwari, M.K. Joshi, Technological trends in heavy metals removal from industrial wastewater: a review, J. Environ. Chem. Eng. 9 (4) (2021) 105688.
- [14] A. Azimi, A. Azari, M. Rezakazemi, M. Ansarpour, Removal of heavy metals from industrial wastewaters: a review, ChemBioEng Rev. 4 (1) (2017) 37–59.
- [15] J.A. Buledi, S. Amin, S.I. Haider, M.I. Bhanger, A.R. Solangi, A review on detection of heavy metals from aqueous media using nanomaterial-based sensors, Environ. Sci. Pollut. Control Ser. 28 (2021) 58994–59002.
- [16] C. Duan, T. Ma, J. Wang, Y. Zhou, Removal of heavy metals from aqueous solution using carbon-based adsorbents: a review, J. Water Process Eng. 37 (2020) 101339.
- [17] C. Duan, T. Ma, J. Wang, Y. Zhou, Removal of heavy metals from aqueous solution using carbon-based adsorbents: a review, J. Water Process Eng. 37 (2020) 101339.
- [18] R. Janani, B. Gurunathan, K. Sivakumar, S. Varjani, H.H. Ngo, E. Gnansounou, Advancements in heavy metals removal from effluents employing nano-adsorbents: way towards cleaner production. Environ. Res. 203 (2022) 111815.
- [19] A. Abbas, A.M. Al-Amer, T. Laoui, M.J. Al-Marri, M.S. Nasser, M. Khraisheh, M. A. Atieh, Heavy metal removal from aqueous solution by advanced carbon nanotubes: critical review of adsorption applications, Separ. Purif. Technol. 157 (2016) 141–161.
- [20] S. Velusamy, A. Roy, S. Sundaram, T. Kumar Mallick, A review on heavy metal ions and containing dyes removal through graphene oxide-based adsorption strategies for textile wastewater treatment, Chem. Rec. 21 (7) (2021) 1570–1610.
- [21] N.I. Zaaba, K.L. Foo, U. Hashim, S.J. Tan, W.W. Liu, C.H. Voon, Synthesis of graphene oxide using modified hummers method: solvent influence, Procedia Eng. 184 (2017) 469–477.

- [22] C.Y. Hsu, A.M. Rheima, M.S. Mohammed, M.M. Kadhim, S.H. Mohammed, F. H. Abbas, Z.H. Mahmoud, Application of carbon nanotubes and graphene-based nanoadsorbents in water treatment, BioNanoScience (2023) 1–19.
- [23] National Center for Biotechnology Information, PubChem compound summary for CID 70120, 6-aminouracil, Retrieved November 25, 2023 from, https://pubchem. ncbi.nlm.nih.gov/compound/6-Aminouracil, 2023.
- [24] National Center for Biotechnology Information, PubChem compound summary for CID 3301, ethylenediamine, Retrieved November 25, 2023 from, https://pubchem. ncbi.nlm.nih.gov/compound/Ethylenediamine, 2023.
- [25] H.N.K. Al-Salman, M. sabbar Falih, H.B. Deab, U.S. Altimari, H.G. Shakier, A. H. Dawood, E. Kianfar, A study in analytical chemistry of adsorption of heavy metal ions using chitosan/graphene nanocomposites, Case Stud. Chem. Environ. Eng. 8 (2023) 100426.
- [26] H.K. Jeong, Y.P. Lee, R.J. Lahaye, M.H. Park, K.H. An, I.J. Kim, Y.H. Lee, Evidence of graphitic AB stacking order of graphite oxides, J. Am. Chem. Soc. 130 (4) (2008) 1362–1366
- [27] S. Wang, H. Sun, H.M. Ang, M.O. Tadé, Adsorptive remediation of environmental pollutants using novel graphene-based nanomaterials, Chem. Eng. J. 226 (2013) 336–347
- [28] N. Van Nguyen, V. Pirouzfar, R. Chidan, Water saving and decreasing make-up water consumption according to industrial wastewater treatment systems, including brine evaporator, crystallizer, and adiabatic processes, Int. J. Energy Water Resour. (2024) 1–17.
- [29] V. Fakhri, A. Jafari, F.L. Vahed, C.H. Su, V. Pirouzfar, Polysaccharides as ecofriendly bio-adsorbents for wastewater remediation: current state and future perspective, J. Water Process Eng. 54 (2023) 103980.
- [30] R. Sarmadi, M. Salimi, V. Pirouziar, The assessment of honeycomb structure UiO-66 and amino functionalized UiO-66 metal-organic frameworks to modify the morphology and performance of Pebax® 1657-based gas separation membranes for CO2 capture applications, Environ. Sci. Pollut. Control Ser. 27 (2020) 40618–40632.
- [31] V. Pirouzfar, S.N. Moghaddam, S.A.H.S. Mousavi, A.H.S. Dehaghani, H. Mollabagher, C.H. Su, Investigation of light aromatics removal from industrial wastewater using nano metal organic framework, J. Contam. Hydrol. 249 (2022) 10048
- [32] V. Pirouzfar, N. Roustaie, C.H. Su, Gas transport characteristics of mixed matrix membrane containing MIL-100 (Fe) metal-organic frameworks and PEBAX precursors, Kor. J. Chem. Eng. 40 (9) (2023) 2138–2148.
- [33] F. Arjomandi Rad, J. Talat Mehrabad, M. Dizaji Esrafili, A communal experimental and DFT study on structural and photocatalytic properties of nitrogen-doped TiO2, Adv. J. Chem., Sec. A 6 (3) (2023) 244–252, https://doi.org/10.22034/ aica.2023.391772.1358.
- [34] A.M. Ayuba, T.A. Nyijime, S.A. Minjibir, F. Iorhuna, 'Adsorption monitoring of triflouroaceticacid, pentadecyl ester and pentadecanoic acid, 14-methyl-, methyl ester on Fe (110): using DFT and molecular simulation', Eura. J. Sci. Technol. 4 (2) (2024) 105–116, https://doi.org/10.48309/eist.2024.423518.1108.
- [35] T. Hadadi, M. Shahraki, P. Karimi, Methane, chlorofluorocmethane and chlorodifluoromethane adsorption onto graphene and functionalized graphene sheets: computational methods, Asian J. Green Chem. 8 (6) (2024) 652–671, https://doi.org/10.48309/AIGC.2024.464931.1528
- [36] M. Kamali-Ardakani, E. Rostami, A. Zare, 'Graphene Oxide@Polyaniline-FeF3 (GO@PANI-FeF3) as a novel and effectual catalyst for the construction of 4H-Pyrimido[2,1-b]benzothiazoles', Adv. J. Chem., Sec. A 7 (3) (2024) 236–247, https://doi.org/10.48309/ajca.2023.428749.1460.
- [37] S.M. Marvast, E. Rostami, 'Graphene oxide modified with tetramethylethylenediamine ammonium salt as a powerful catalyst for production of trisubstituted imidazoles', Asian J. Green Chem. 8 (3) (2024) 261–277, https:// doi.org/10.48309/aigc.2024.430848.1469.
- [38] N. Musheer, M. Yusuf, A. Choudhary, M. Shahid, Recent advances in heavy metal remediation using biomass-derived carbon materials, Adv. J. Chem., Sec. B: Nat. Product Med. Chem. 6 (3) (2024) 284–345, https://doi.org/10.48309/ aicb.2024.462275.1235.
- [39] F.H. Saboor, A. Ataei, Decoration of metal nanoparticles and metal oxide nanoparticles on carbon nanotubes, Adv. J. Chem., Sec. A 7 (2) (2024) 122–145, https://doi.org/10.48309/ajca.2024.416693.1420.
- [40] S. Sajjadifar, F. Abakhsh, Z. Arzehgar, Design and characterization of Fe<sub>3</sub>O<sub>4</sub>@n-pr-NH<sub>2</sub>@Zn<sub>3</sub>(BTC)<sub>2</sub> magnetic MOF: a catalyst for dihydropyrimidine and 2-amino-4H-chromene synthesis, Chem. Methodol. 8 (8) (2024) 550–568, https://doi.org/10.48309/chemm.2024.472969.1817.

- [41] L. Yang, J. Liang, Z. Liu, J. Yuan, G. He, Hierarchical micro/nano-architected nylon mesh integrated with metal-organic framework, cellulose nanocrystal, and graphene oxide for high-efficient oil-water separation, J. Appl. Polym. Sci. 142 (24) (2025) e57010.
- [42] A.S. Khan, P. Srivastava, Challenges and future perspectives in nanotechnology for sustainable water and wastewater management, in: Nano-solutions for Sustainable Water and Wastewater Management: from Monitoring to Treatment, Springer Nature Switzerland, Cham, 2025, pp. 469–492.
- [43] N. Sikri, S. Kumar, B. Behera, J. Mehta, Graphene oxide/layered double hydroxide composite as highly efficient and recyclable adsorbent for removal of ciprofloxacin from aqueous phase, Front. Nanotechnol. 7 (2025) 1578620.
- [44] A.K. Dutta, Carbon-based metal-free nano-materials: an alternative next-generation innovative material for future, in: Innovative Materials for Next-Generation Defense Applications: Cost, Performance, and Mass Production, IGI Global Scientific Publishing, 2025, pp. 35–60.
- [45] S. Tajik, F. Garkani Nejad, R. Zaimbashi, H. Beitollai, Voltammetric sensor for acyclovir determination based on MoSe2/rGO nanocomposite modified electrode, Chem. Methodol. 8 (5) (2024) 316–328, https://doi.org/10.48309/ chemp. 2024.444547 1771
- [46] R. Zainul, R. Rafika, H. Hasanudin, I.A. Laghari, D.M.H. Hamdani, J. Mapanta, R. Handayana, D. Delson, R.S. Mandeli, H. Putra, M.S.B. Sravan, A. Azril, A. A. Adeyi, S. Saefulloh, Systematic review of electrochemical stability and performance enhancement in energy storage and analytical applications, Asian J. Green Chem. 8 (2) (2024) 198–216, https://doi.org/10.48309/ aigc.2023.426701.1465.
- [47] E. Padilla-Ortega, R. Leyva-Ramos, J. Flores-Cano, Binary adsorption of heavy metals from aqueous solution onto natural clays, Chem. Eng. J. 225 (2013) 535–546
- [48] V.C. Srivastava, I.D. Mall, I.M. Mishra, Removal of cadmium (II) and zinc (II) metal ions from binary aqueous solution by rice husk ash, Colloids Surf. A Physicochem. Eng. Asp. 312 (2–3) (2008) 172–184.
- [49] V. Chandra Srivastava, I. Deo Mall, I. Mani Mishra, Modelling individual and competitive adsorption of cadmium (II) and zinc (II) metal ions from aqueous solution onto bagasse fly ash, Separ. Sci. Technol. 41 (12) (2006) 2685–2710.
- [50] H.E. Reynel-Avila, D.I. Mendoza-Castillo, A.A. Olumide, A. Bonilla-Petriciolet, A survey of multi-component sorption models for the competitive removal of heavy metal ions using bush mango and flamboyant biomasses, J. Mol. Liq. 224 (2016) 1041–1054.
- [51] Q. Zeng, K. Chen, X. Huang, S. Luo, X. Wang, D. Luo, C. Chen, Competitive adsorption of oxytetracycline and sulfamethoxazole by nanosized activated carbon in aquatic environments: experimental analysis and DFT calculations, Chem. Eng. J. 499 (2024) 156375.
- [52] L.A. Gallego-Villada, W.Y. Perez-Sena, J.E. Sánchez-Velandia, J. Cueto, M. del Mar Alonso-Doncel, J. Wärmå, D.Y. Murzin, Synthesis of dihydrocarvone over dendritic ZSM-5 Zeolite: a comprehensive study of experimental, kinetics, and computational insights, Chem. Eng. J. 498 (2024) 155377.
- [53] X. Wang, A. Hussain, H. Zhu, Y. Li, X. Wang, D. Li, Simultaneous adsorption of multi-heavy metal ions from wastewater via grafted phosphate functionality on polyvinyl alcohol, Water, Air, Soil Pollut. 234 (10) (2023) 638.
- [54] N.A. Qasem, R.H. Mohammed, D.U. Lawal, Removal of heavy metal ions from wastewater: a comprehensive and critical review, npj Clean Water 4 (1) (2021) 1–15
- [55] Z. Wang, W. Xu, F. Jie, Z. Zhao, K. Zhou, H. Liu, The selective adsorption performance and mechanism of multiwall magnetic carbon nanotubes for heavy metals in wastewater, Sci. Rep. 11 (1) (2021) 16878.
- [56] D.B. Olawade, O.Z. Wada, B.I. Egbewole, O. Fapohunda, A.O. Ige, S.O. Usman, O. Ajisafe, Metal and metal oxide nanomaterials for heavy metal remediation: novel approaches for selective, regenerative, and scalable water treatment, Front. Nanotechnol. 6 (2024) 1466721.
- [57] J. Wang, G. Zhao, Y. Li, H. Zhu, X. Peng, X. Gao, One-step fabrication of functionalized magnetic adsorbents with large surface area and their adsorption for dye and heavy metal ions, Dalton Trans. 43 (30) (2014) 11637–11645.
- [58] A. Jawed, A. Sharad, A. Chutani, L.M. Pandey, Amine functionalized Fe (III)-doped-ZnO nanoparticles based alginate beads for the removal of Cu (II) from aqueous solution, Nano-Struct. Nano-Objects 38 (2024) 101199.
- [59] M.T. De Araujo, J.W. De M. Carneiro, A.G. Taranstlto, Solvent effects on the relative stability of radicals derived from artemisinin: DFT study using the PCM/ COSMO approach, Int. J. Quant. Chem. 106 (13) (2006) 2804–2810.